International Journal of Pharmaceutics 682 (2025) 125976

Contents lists available at ScienceDirect

International Journal of Pharmaceutics

journal homepage: www.elsevier.com/locate/ijpharm

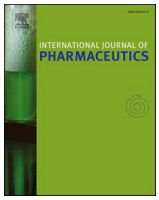

Guiding excipient selection for amorphous solid dispersions by combining an in vitro-in-silico approach – II: Supersaturation and drug release

Egis Zeneli [a,b,c], Hugo Bohets [c], Frédéric Ngono Mebenga [c], Christophe Tistaert [c], René Holm [d], Martin Kuentz [b,*]

[a] University of Basel, Department of Pharmaceutical Sciences, Klingelbergstrasse 50, 4056 Basel, Switzerland
[b] University of Applied Sciences and Arts Northwestern Switzerland, Institute of Pharma Technology Hofackerstr. 30, CH-4132 Muttenz, Switzerland
[c] Janssen Phramaceutica, Turnhoutseweg 30, 2340 Beerse, Belgium
[d] University of Southern Denmark, Department of Physics, Chemistry and Pharmacy Campusvej 55, 5230 Odense, Denmark

ARTICLE INFO

Keywords:
ASD dissolution
Precipitation inhibition
High-throughput
COSMO-RS
In vitro/in silico alignment

ABSTRACT

There is a growing industrial need for quick and early screening of amorphous solid dispersions (ASDs). While new technologies are emerging, including in-silico predictions and high-throughput experimentation, a significant gap exists due to a lack of comparative data. The aim of this work was thus to compare experimental data with calculations obtained by the Conductor like Screening Model for Real Solvents (COSMO-RS). A small-scale high throughput method based on solvent casting was used to evaluate the release behavior and precipitation inhibition capacity of ASDs of griseofulvin and nifedipine in the presence of ten pharmaceutically relevant polymers. COSMO-RS was then used to investigate the interaction strength between drug and polymer by means of drug activity coefficients. A stronger interaction would result in better supersaturation maintenance. This was reflected in our results and a good alignment between calculations and experimental performance was observed. COSMO-RS effectively differentiated between polymers with strong precipitation inhibition (PI) functionality and separated those with weaker efficacy for most of the ASDs studied. This pre-selected list of polymers can serve as a foundation for additional studies on all relevant drug development quality attributes, from stability to manufacturing.

1. Introduction

1.1. Polymer selection in amorphous solid dispersions

An increasing number of new active pharmaceutical ingredients (APIs) in modern drug discovery exhibit poor water solubility, which can negatively affect their absorption (Kawakami, 2012). The extent of drug absorption via the oral route primarily depends on three factors: solubility, dissolution rate, and intestinal permeability. The preparation of amorphous solid dispersions (ASDs) offers a promising solution to dissolution and absorption challenges (Zhang et al., 2019, Wolbert et al., 2022; Rumondor et al., 2009). ASDs are systems in which the API is dispersed within a polymeric matrix; due to their high free energy they can significantly improve the apparent aqueous solubility relative to the compound's thermodynamic solubility (Taylor, 2016). Additionally, the presence of polymeric carriers can improve API wetting, further enhancing dissolution rate and oral absorption. Selecting the right polymeric carrier is key to obtaining the desired API release from the formulation, delaying precipitation in vitro and in vivo, as well as enabling an acceptable shelf life (Wyttenbach et al., 2013). The choice of polymer can greatly influence the dissolution behavior of an ASD by affecting the dissolution rate as well as the amount of dissolved drug, both of which are key for effective administration within the gastrointestinal transit time (Fdukeck et al., 2013). Besides the drug dissolution kinetics influenced by the polymer, several other aspects must be investigated to ensure good performance of the final formulation. After early pre-formulation and profiling of drug candidates, different ASD screening assays can be carried out to select candidate excipients that meet several formulation requirements. Early ASD development screening may be oriented towards aspects such as apparent solubility, physical stability and supersaturation maintenance to reach early-phase clinical trials. At a later stage, further quality aspects such as manufacturability, long-term physical stability, regulatory requirements and cost-of-goods have to be considered. For example, API-polymer

* Corresponding author..
E-mail address: martin.kuentz@fhnw.ch (M. Kuentz).

https://doi.org/10.1016/j.ijpharm.2025.125976
Received 19 May 2025; Received in revised form 2 July 2025; Accepted 14 July 2025
Available online 15 July 2025

miscibility should be considered at an early stage, as it is generally a prerequisite for physical stability. Another key factor is solubility and potential amorphous drug loading of the API in the polymer, as this affects the degree of supersaturation, possibly supersaturation maintenance due to drug affinity to the polymer, and finally the achievable dose strength. Here, the development stage and drug availability play key roles. For instance, larger quantities of API and polymer are needed for formulation development and supply in later stages of clinical development. Amorphous solid dispersions are typically produced through hot melt extrusion, spray drying or, less commonly, lyophilization (Han et al., 2023; Baird and Taylor, 2012). Each of these manufacturing methods comes with specific requirements for the polymer, as outlined in the literature (Bhujbal et al., 2021). Furthermore, the pH profile of the polymer may be important, especially when an enteric polymer is required for targeted release. Another point to consider is API permeability: good permeability leads to rapid drug absorption. In such cases, maintaining supersaturation for long periods of time may not be as critical as for less permeable drugs or when the dose is relatively low. In summary, while polymer selection for a final drug product has to be based on multiple formulation parameters, an early-stage ASD screening assay can focus on a specific performance factor such as drug supersaturation, which was the focus of the present work.

1.2. Novel tools to support early development of amorphous formulations

High throughput screening methods are increasingly used in the pharmaceutical field, which has greatly facilitated screening not just in drug discovery but also in early formulation development, for example to identify suitable polymers in supersaturating formulations (Dai et al., 2007; Warren et al., 2010). Miniaturized ASD screening is becoming more established in pharmaceutical firms, and solvent casting is typically employed for subsequent physical and chemical analysis (Chiang et al., 2012; Shanbhag et al., 2008). Nevertheless, selecting the appropriate excipient remains a time-consuming and costly process, often constrained by limited API availability, especially in the early stages of development (Wyttenbach et al., 2013). This emphasizes the need for non-empirical methods such as computational models to help guide excipient selection, and such computational methods have gained wide attention in the pharmaceutical field to support drug development. Molecular dynamics simulations (MDs), for instance, have often been used to gain mechanistic understanding of drug-excipient interactions in ASDs (Aulifa et al., 2024; Xiang and Anderson, 2014). Ditzinger et al used MDs to gain structural insights into the interaction between fenofibrate, lysine and sodium-CMC as extruded ASD formulations (Ditzinger et al., 2020). Apart from such force-field based molecular simulations, the conductor-like screening model for real solvents (COSMO-RS) is of particular interest as it combines quantum-chemical surface calculations with statistical thermodynamics (Klamt and Eckert, 1999). In a study by Price and colleagues, COSMO-RS as a fragment-based approach, has been successfully used to select precipitation inhibitors (Price et al., 2019). More recently, COSMO-RS was employed for ternary ASDs and Antolovic and co-workers utilized COSMO-SAC (Segment Activity Coefficient) to predict the compatibility between APIs and polymers (Antolovic et al., 2024; Niederquell et al., 2024). The latter research incorporated both the solubility and miscibility of the API with the polymer, finding that while the model tended to slightly overestimate API solubility in the polymer, the overall predictions were reasonable (Antolovic et al., 2024). From a qualitative perspective, the model also correctly ranked polymers based on their API compatibility. The aim of the present study was therefore to evaluate COSMO-RS as a support tool for high-throughput screening methods, to guide excipient selection in the early stages of ASD development.

2. Materials and methods

2.1. Materials

Nifedipine was purchased from Thermo Fisher Scientific (Dreieich, Germany). Griseofulvin was purchased from Sigma-Aldrich (Darmstadt, Germany). Purity for both APIs was 98 %. Hydroxypropyl methylcellulose acetate succinate (HPMC AS) grades LG, MG and HG were purchased from Shin Etsu AQOAT (Chigasaki, Japan), Eudragit grades E100 and L100 were obtained from Evonik (Essen, Germany), Soluplus, polyvinylpyrrolidone K30 (PVP K30) and polyvinylpyrrolidone vinyl acetate 64 (PVP VA 64) were purchased from BASF (Ludwigshafen, Germany) and hydroxypropyl methylcellulose (HPMC) E5 was obtained from VWR (Leuven, Belgium). Dichloromethane, methanol, formic acid, glacial acetic acid, tris base, hydrochloric acid and sodium hydroxide were purchased from Merck (Darmstadt, Germany). Sodium chloride, maleic acid and isopropanol were from VWR (Leuven, Belgium). N-methylpyrrolidone (NMP) was purchased from Sigma-Aldrich (Darmstadt, Germany). Finally, trifluoroacetic acid (TFA) was obtained from Thermo Scientific (Ghent, Belgium).

2.2. Methods

2.2.1. Preparation of amorphous solid dispersions

ASDs of griseofulvin and nifedipine were film casted in combination with ten pharmaceutically relevant polymers. Drug stock and polymer stock solutions were prepared separately in dichloromethane:methanol solvent mixture 1:1 (v/v). Subsequently, the polymer and API stock were used to prepare API:polymer master mixes in a 1:2 and 1:3 (v/v) ratio using the Hamilton Microlab STAR liquid handling robot (Bonheiden, Belgium). Nifedipine is a light sensitive compound and was protected from light whenever possible. 777 μg films were casted in 10 mL headspace glass vials (46x22.5 mm, clear glass) from VWR (Leuven, Belgium) to eventually yield 100 μg films after addition of 7 mL media during the release assay. Casting was followed by quick solvent evaporation at 70 °C under vacuum for one hour in a Heraeus Vacutherm oven from Thermo Scientific (Dreieich, Germany). All samples were cast in triplicate. The present study is a continuation of our previous work (Zeneli at al., 2025) and amorphousness of the ASD films was verified as part of such screening.

2.2.2. Drug release assay

A single phase, non-sink, miniaturized high-throughput dissolution test was conducted in blank simulated fasted state intestinal fluid (FaSSIF), i.e., without lecithin and taurocholate, (pH 6.5) for the tested ASDs. Seven mL of fresh media, preheated at 37 °C, was added to the films and samples were shaken at 37 °C using the Hamilton Microlab STAR liquid handling robot (Bonheiden, Belgium); the samples were then incubated for two hours. 500 μL of mixture were collected and transferred to a preheated polytetrafluoroethylene (PTFE) filter plate at each time point. 100 μL of filtrate were transferred to a Nunc (A/S) ultra performance liquid chromatography (UPLC) 96 well block from Sigma Aldrich (Steinheim, Germany) and diluted with 100 % NMP prior to drug quantification. The blocks were immediately sealed with pre-slit well caps from Thermo Scientific (Dreieich, Germany).

2.2.3. Equilibrium solubility

Equilibrium solubility of griseofulvin was determined in blank FaSSIF, pH 6.5, in absence of polymer, using the Hamilton Microlab STAR liquid handling robot. Excess drug was transferred to Nunc 2 mL 96 deep-well blocks from Sigma Aldrich (Steinheim, Germany). The blocks were sealed and incubated under shaking at 37 °C for 24 h. 500 μL of mixture were collected and transferred to a preheated PTFE filter plate. 100 μL of filtrate were transferred to a Nunc (A/S) UPLC 96 well block and diluted with 100 % NMP prior to drug quantification. The blocks were immediately sealed with pre-slit well caps for PP plate from

Thermo Scientific (Dreieich, Germany). Nifedipine quantification was not successful with this method, which suggested that the miniaturized drug separation method may have caused some loss of quantifiable drug in solution. Therefore, measurements were in this case repeated at a larger 10 mL scale.

2.2.4. UPLC quantification of the APIs

Samples were separated on an Acquity UPLC BEH C18 column (2.1 x 50 mm, 1.7 μm particle size) from Waters™ (Etten-Leur, Netherlands). The mobile phase was composed of 0.1 % (v/v) TFA in water (A) and acetonitrile (B), respectively, for both griseofulvin and nifedipine. The instrument flow rate was set to 0.6 mL/min with a run time of 3.5 min per injection. Griseofulvin was detected at a wavelength of 293 nm, while nifedipine was measured at 236 nm, using an Acquitiy UPLC® BEH C18 1.5 μm column and an injection volume of 2 μL.

2.2.5. COSMO-RS modelling

COSMO-RS (Conductor-like Screening Model for Real Solvents) is based on the conductor-like screening model (COSMO) and has been well described in the literature (Klamt and Eckert, 1999; KLAMT, 2011). It belongs to the family of dielectric continuum solvation models, particularly related to polarizable continuum models (PCM), but offers several advantages. Unlike classical PCM models, COSMO-RS can distinguish between solvents with identical dielectric constants. Moreover, it enables consistent thermodynamic predictions for mixtures over a broad temperature range, extending the applicability of continuum models to systems that were previously inaccessible (Diedenhofen and Klamt, 2010; Klamt and Eckert, 1999). COSMO-RS combines quantum chemical calculations with statistical thermodynamics to predict key thermodynamic properties, such as solubility and molecular interactions in solvents. In this framework, the solvent is modeled as a continuous dielectric medium in which solute molecules are embedded. This medium shields the solute's charge distribution, influencing solvation energies and solute–solvent interactions.

Fig. 1 shows the screening charge densities of the model drugs griseofulvin and nifedipine; similarly, a solvent S can also be represented. Notably, COSMO surface charges typically have inverted signs compared to the original electron density. Regions of higher electron density correspond to more positive screening charge density, while regions of lower density correspond to more negative screening charge density. Solvent–solute interactions are modeled as a collection of interacting surface segments, with the interaction energy between each segment pair defined by their respective screening charge densities (σ and σ′). For a more detailed explanation of the statistical thermodynamic framework, see Klamt and Eckert (2000).

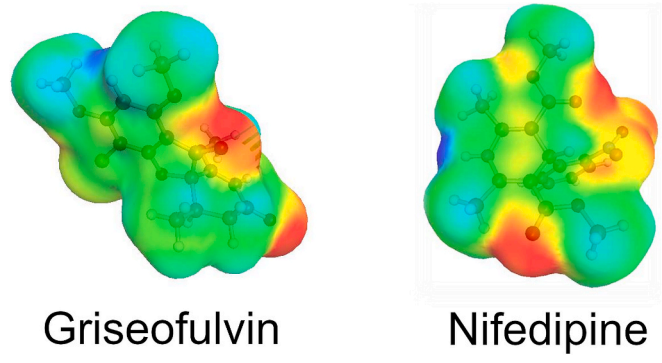

Fig. 1. Sigma surface of griseofulvin and nifedipine with color-coded screening charge density from red (corresponding to high electron density) over green (corresponding to neutral surface charge) to blue (indicating a low electron density). (For interpretation of the references to color in this figure legend, the reader is referred to the web version of this article.). (For interpretation of the references to color in this figure legend, the reader is referred to the web version of this article.)

In the final step, activity coefficients ($\ln \gamma_j$) were calculated using the COSMOthermX software from BIOVIA (Dassault Systèmes Germany GmbH, Leverkusen, Germany; version 22.0.0) using the following relation:

$$\ln\left(\gamma_j\right) = \frac{\left(\mu_j^{(i)} - \mu_j^{(P)}\right)}{RT}$$

where, $\mu_j^{(P)}$ is the pseudo-chemical potential of the pure component j and $\mu_j^{(i)}$ is the pseudo-chemical potential of the component j in the liquid phase.

For more computational details on molecular models, the 3D geometry of each API was generated from their SMILES code and a geometry optimization of the molecule was then performed using the Forcite module (Material Studio, release 2024) with ultra-fine convergence criteria. This optimized geometry was later used to compute screening charge densities of the APIs using the TURBOMOLE software package (version 7.4), employing the Becke-Perdew (BP86) density functional (Perdew, 1986; Becke, 1988) with the triple-zeta valence polarized (TZVP) basis set (BP-TZVP-COSMO + GAS_18 template as implemented in COSMOconf). Most of the conformations generated were within a relative energy ranking of 3 kcal/mol and were all considered for activity coefficient calculation.

Moreover, polymer screening charge densities were also generated at the BP-TZVP-COSMO level. To construct polymer models, COSMOconf calculations were performed on trimers of the different oligomeric units comprising the polymer. These trimers were merged into a single.mcos file representative of the polymer, with weight fractions of each oligomer assigned based on the polymer's chemical composition.

3. Results and discussion

3.1. Release assay and equilibrium solubility assessment

To determine the impact of the buffer on API solubility, a 24 h equilibrium solubility assay in blank FaSSIF, pH 6.5, was conducted. Crystalline equilibrium solubility of the two APIs was found to be 10.45 μg/mL and 7.43 μg/mL for griseofulvin and nifedipine respectively. This was in line with solubilities reported from other groups (Plumley et al., 2009; Ding et al., 2023). Furthermore, to evaluate the dissolution profile of the ASDs studied, a one-phase, non-sink, high-throughput release assay was carried out in blank FaSSIF (i.e., without lecithin and taurocholate), pH 6.5. The release kinetics of the film can play a significant role in drug absorption, depending on the API permeability properties. Therefore, understanding the maximum drug supersaturation (i.e. "spring" effect) and the ability to sustain such metastable drug solutions (i.e. "parachute" effect) represent crucial performance characteristics of an ASD (Guzman et al.,2007). For this study, it was not intended to link calculations with the spring effect due to an incomplete understanding of drug-dependence, whereas the precipitation inhibition appeared computationally more accessible as outcome of drug-excipient interaction. Therefore, the study focused on investigating the alignment between calculations and the precipitation inhibition performance of the polymers. This aspect will be discussed in more detail in the following sections. Dissolution profiles for griseofulvin and nifedipine ASDs are presented in Fig. 2.

The Eudragit and HPMC AS families of polymers were expected to exhibit pH-dependent release owing to their respective functional groups. Specifically, HPMC AS LG dissolves at pH values above 5.5, HPMC AS MG at pH above 6, and HPMC AS HG at pH above 6.5. Furthermore, HPMC AS HG is the most hydrophobic of the three grades (Butreddy, 2022). The pH-dependent release, along with the higher viscosity of HPMC AS HG and its hydrophobicity, was likely responsible for its slower release rate compared to the other two HPMC AS polymers observed in Fig. 2 (Butreddy, 2022). Similarly, Eudragit E100 and L100

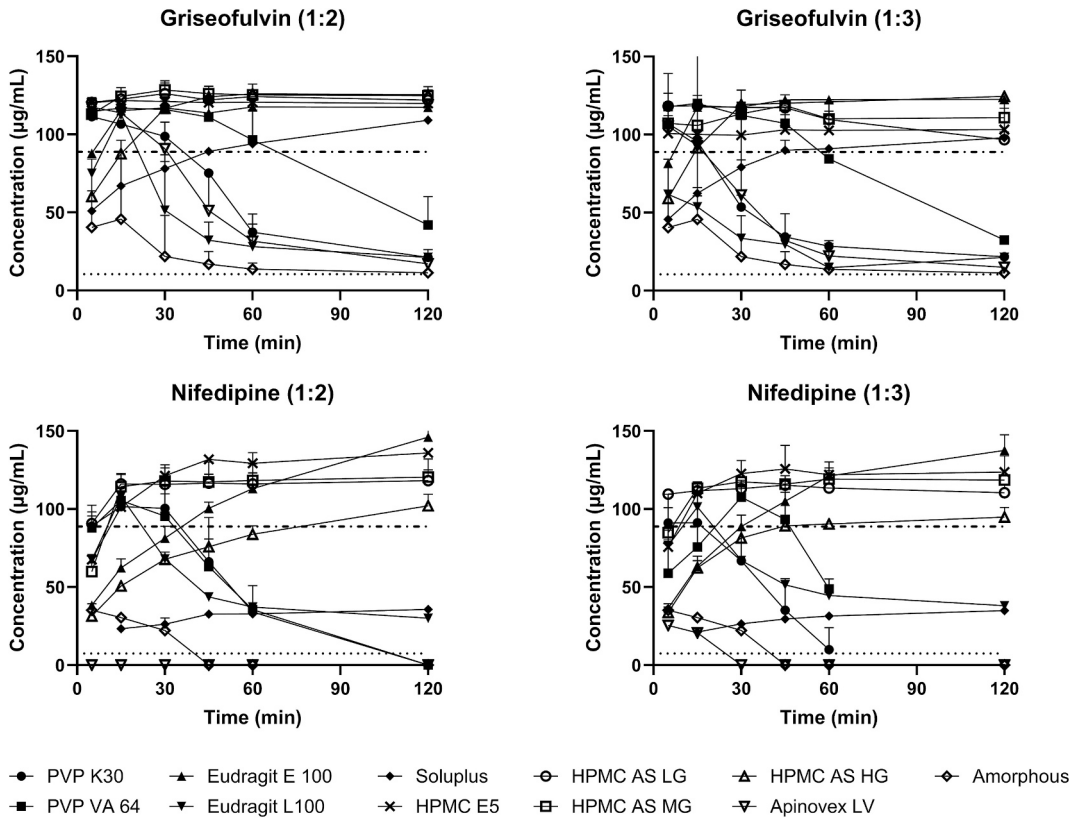

Fig. 2. Dissolution profile of the amorphous solid dispersions, ASDs studied, in blank FaSSIF (buffer without bile salts or phospholipids), pH 6.5. 1:2 (w/w) and 1:3 (w/w) represent the drug:polymer composition ratio of the ASD. Where curves drop to zero, the value was below the experimental detection limit of 0.05 µg/mL for griseofulvin and 0.5 µg/mL for nifedipine. Dotted lines correspond to the thermodynamic equilibrium solubility of the studied drugs. Dashed lines correspod to 80% API released from the ASDs.

are also known to exhibit a pH-dependent release, with Eudragit E100 expected to best dissolve below pH 5 (Linares et al., 2019). In our experiments, it dissolved within the first 5 min of the drug release test and maintained supersaturation throughout the entire experiment. Eudragit E100 has also been reported to dissolve at and above pH 6.5 also in other studies (Chauhan et al., 2013; Leopold and Eikeler, 1997). The latter also studied the dissolution behavior of dexamethasone tablets in presence and absence of Eudragit E100 coating in acidic and basic media. It was observed that in acidic medium, drug release was initiated by dissolution of the polymer film, whereas in basic medium, drug release was due to swelling of the tablet core and consequent polymer film disruption (Leopold and Eikeler, 1997). In the present work, blank FaSSIF pH 6.5, was used for the release experiments. Although determining the release mechanism was outside the scope of the study, it is likely that, similarly to the work presented by Leopold and coworkers, drug release was driven by the hydration of the polymer film. Such hydration and erosion of the polymer film together with drug-polymer interactions has often been demonstrated to govern at least the initial drug release from ASDs (Chen et al., 2016). Mechanistically, the interplay of components in the evolving hydration layer is crucial. At high drug loading, when the limit of congruency is reached, deviations from a hydration-driven release are expected, leading to complex phase separation and making drug-excipient interactions particularly intricate (Que et al., 2021). Thus, depending on drug and polymer, drug-rich phases and separation have been shown experimentally to occur in the hydration layer, thereby greatly reducing the apparent release rates (Frank et al., 2022).

PVPs, HPMC E5, Soluplus, and Apinovex were expected to have a practically pH-independent release profile, with Soluplus being the slowest to release the drug (Fig. 2). Soluplus is a large, grafted copolymer, composed of polyethylene glycol, polyvinyl caprolactam and polyvinyl acetate with a molecular weight ranging from 90,000 to 140,000 g/mol (Alopaeus, 2019). It is possible that at least the initial polymeric hydration of Soluplus could have been slower compared to other polymers of lower molecular weight such as PVP K30 (MW 40,000 g/mol) thereby causing reduced initial release kinetics.

To compare precipitation inhibition capacity across the different polymers, only those that showed no precipitation and that reached at least 80 % dissolution were carried forward for comparison after the initial analysis. This corresponded to an apparent supersaturation level of 8.5 for griseofulvin and 11.9 for nifedipine, compared to the equilibrium solubility of the APIs in blank FaSSIF. Where, the term apparent supersaturation is defined as the ratio between the concentration of drug in the supersaturated solution according to the experimental methodology and the thermodynamic solubility of the crystalline drug. Given the variety and number of polymers evaluated in this study, along with the differences in observed supersaturation levels, it was necessary to establish a defined range for comparison purposes. It is well known that the supersaturation level is the driving force for precipitation, resulting in increased nucleation and crystal growth rates (Chauhan et al., 2013). Thus, having comparable levels of supersaturation within the ASDs with the same API was key. Two drug to polymer ratios were studied and results can be seen in Fig. 3.

When examining the release profiles of both griseofulvin and nifedipine ASDs, some initial supersaturation was generally achieved as a spring effect (Guzman et al., 2007). Even neat amorphous API offered such a distinct solubility advantage for about 30 min. After 30 min the concentration was reduced to that close to the thermodynamic solubility of the compounds, also shown in Fig. 2. The required time window of increased supersaturation in vivo generally depends on a drug's permeability and dose. Whenever sustained supersaturation is required, there is a need for precipitation inhibition by excipients. When

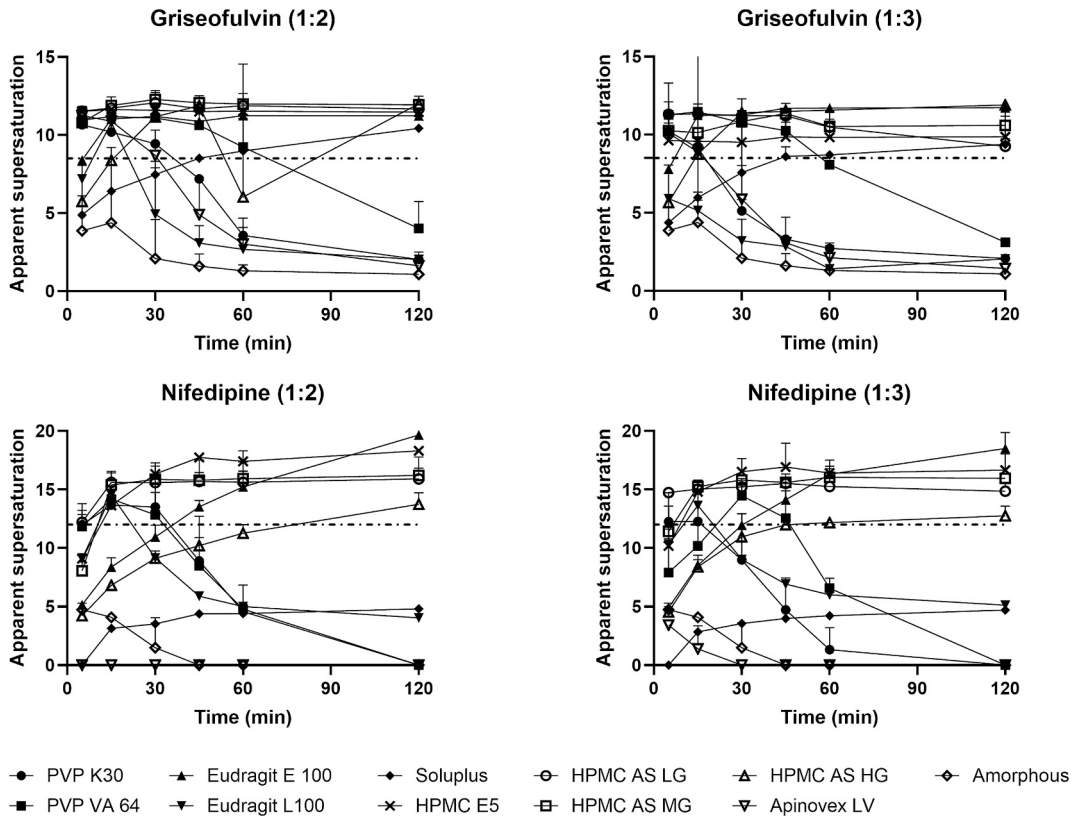

Fig. 3. Apparent supersaturation of the studies ASDs in blank FaSSIF, pH 6.5. 1:2 (w/w) and 1:3 (w/w) represent the drug:polymer composition ratio of the ASD. Where curves drop to zero, the value was below the experimental detection limit of 0.05 μg/mL for griseofulvin and 0.5 μg/mL for nifedipine. Dotted lines correspond to 80 % drug released from the ASD. Dashed lines correspond to 80% API released from the ASDs.

examining such precipitation inhibition capacity of the polymers tested, a distinction was proposed between cellulosic and non-cellulosic polymers, for at least the given model compounds. Our results suggested that the cellulosic polymers, along with Eudragit E100, were the most effective at maintaining high drug concentrations. They were ranked top for precipitation inhibition capacity for ASDs composed of both griseofulvin and polymer, and nifedipine and polymer. Several research groups have investigated the impact of cellulosic polymers on precipitation inhibition, emphasizing their surface-active properties (Chauhan et al., 2013; Gao et al., 2009; Warren et al., 2010). It has been highlighted that HPMC-based polymers can adsorb onto the surface of aggregating nuclei, inhibiting crystal growth by functioning as a mechanical barrier to nucleation (Schram et al., 2015; Gao et al., 2009; Warren et al., 2010; Chauhan et al., 2013; Butreddy, 2022). Drug-polymer interactions have also been shown to play an important role in maintaining high drug concentrations by slowing precipitation, as in the case of Eudragit E 100 (Chauhan et al., 2013; Adhiyaman and Basu, 2006). Chauhan and colleagues studied the infrared spectrum of dipyridamole (DPD) precipitate in presence and absence of Eudragit E100 to evaluate structural changes and possible correlation to supersaturation maintenance. Spectral changes were observed on DPD in presence of polymer compared to DPD alone, indicating that Eudragit E100 delayed precipitation onset and improved supersaturation through API-polymer interactions (Chauhan et al., 2013). More broadly, polymers that exhibit strong API interactions often appear to be the most effective precipitation inhibitors (Chauhan et al., 2013; Warren et al., 2010; Chavan et al., 2016).

In the present study, for ASDs containing griseofulvin, the PVP family of polymers and Apinovex were poorest at maintaining high drug concentrations. On the one hand, the PVPs exhibited a strong initial spring, achieving 80 % dissolution within the first 5 min, followed by a quick decline in concentration after 15 min; eventually reaching equilibrium solubility after 60 min. On the other hand, ASDs containing Apinovex showed both a poor spring and poor parachute effect. While little information is available on the polyacrylic acid excipient Apinovex, it is a highly hydrophilic polymer, similar to PVP K30 and PVP VA. However, the latter have been shown to enhance initial dissolution performance rather than acting as precipitation inhibitors (Knopp et al., 2016).

Regarding nifedipine, similar arguments can be made as for griseofulvin; the best-performing polymers in terms of precipitation inhibition capacity were the HPMC AS family, Eudragit E100 and HPMC E5. In contrast, ASDs comprising PVP K30, PVP VA and Eudragit L100 started precipitation within the first 15 min of the experiment, leaving these polymers at the bottom of the list in terms of precipitation inhibition performance, similar to that observed for griseofulvin. In comparison, Soluplus exhibited a medium supersaturation level, while Apinovex barely affected nifedipine with respect to drug release kinetics. Overall, no significant difference was observed in precipitation inhibition effect between the 1:2 (w/w) and 1/3 (w/w) API:polymer ratios, either for griseofulvin or for nifedipine ASDs. Furthermore, except for the difference in supersaturation level achieved, no difference was observed in PI performance in the presence of the two APIs. Nifedipine ASDs reached a higher level of initial supersaturation than griseofulvin ASDs, despite the lower solubility of nifedipine. This could be explained by the crystallization tendency of these APIs. Griseofulvin is a GFA (glass forming ability) class I compound and a fast crystallizer, while nifedipine is a GFA class II compound and a slower crystallizer (Baird et al., 2010; Alhalaweh et al., 2015). Blaabjerg and colleagues studied the supersaturation propensity and glass forming ability of compounds and proposed a correlation (Blaabjerg et al., 2018). Their work showed that drugs which are good glass formers also had the potential to supersaturate to a high degree, whereas drugs that are modest glass formers would supersaturate only to a comparatively low degree. More data is

needed to support this correlation, and the situation is further complicated by the presence of polymers, as in this work. However, previous research encourages data comparison primarily on a drug-specific basis; and regarding in silico calculations, we considered each drug to polymer ratio separately.

3.2. Ranking of polymers based on COSMO-RS calculations

To obtain a stable ASD formulation, strong interactions between the API and polymer are generally essential (Walden et al., 2021; Zeneli et al., 2025). Similarly, although not the only factor, as outlined in the previous section, stronger API-polymer interactions often enhance supersaturation maintenance, i.e. the parachute effect (Guzman et al., 2007).

Therefore, knowledge of interaction strength between API and polymer in given media can help to identify beforehand polymers that could serve as effective precipitation inhibitors. Different in-silico approaches can be used for this purpose. In this work, we have used API activity coefficient in the solution (containing ASD polymer and dissolution media) calculated using COSMO-RS as an indicator of its affinity with the media. An activity coefficient accounts for deviations from ideal behavior, and it is greatly influenced by molecular interactions. In the present case, a value lower than 1 (corresponding to a negative natural logarithm) indicates favorable (attractive) interactions between the API and its environment, whereas a value higher than 1 (corresponding to a positive natural logarithm) reflects repulsive interactions, typically considered undesirable in this context.

For modeling purposes, the API-polymer ratio was kept constant, while the ASD content in water varied between 1 and 50 % weight. Simultaneously, the water content was decreased from 99 to 50 % weight (Table 1).

It was thereby possible to investigate how changes in water and ASD content may affect interaction strength and ranking of polymers in terms of their effectiveness as precipitation inhibitors. Note that the computed percentage of ASD in solution was only used as a model. Along with changes in water quantity as a function of ASD percentage, it was a possible modeling approach to investigate how dilution could affect interaction between API and polymer, and consequently supersaturation maintenance. Realistic concentrations would result in an inability to detect the interactions due to elevated dilution. COSMO-RS calculation results are presented in Fig. 4.

Table 2 also shows drug activity coefficients for 1 % (w/w) of ASD and 50 % (w/w) ASD content relative to aqueous release medium. The ranking of polymers in the table, from top to bottom, is in order of an increasing activity coefficient suggesting changes towards decreasing interaction strength. Fig. 4 shows that an increase in ASD content, and consequently a decrease in water, resulted in a fall in the calculated drug activity coefficient and therefore an assumed increased interaction strength. This general trend showed the hydrophobic nature of the APIs tested, but also that water can disrupt the binary intermolecular interactions between API and polymer within the limits tested, thus leading to a drug not sufficiently protected by the polymer, which may then favor drug nucleation and crystal growth (Wyttenbach et al., 2013).

Despite an overall decrease in drug activity coefficient with increasing water content, the polymer ranking was essentially unaffected by ASD fraction in solution as seen in Table 2. The only change was observed with a switch in position between Apinovex and Eudragit L100 for the ASD comprising Nifedipine and polymer in a 1:2 ratio. Considering the similarity of calculated activity coefficients and the change by only one position, this could be a bias of the calculations.

3.3. Comparison between in and vitro results and in-silico ranking

One of the objectives of this study was to compare the experimental results with the polymer ranking derived from the computational COSMO-RS calculations. As mentioned earlier, this work was part of a broader screening approach, where physical stability was considered separately (Zeneli et al., 2025). From that perspective, there were two aims: to choose a polymer that was a good precipitation inhibitor, depending on API characteristics; secondly, to pre-select several suitable polymers to facilitate a choice of a suitable carrier that met most quality attributes required of the drug product. This list of attributes beyond drug release may differ from early formulations to final product; it includes physical stability, processability, manufacturability and other project-specific criteria. Meeting all the prerequisites and conducting the required testing within set deadlines and with limited API availability can be very challenging, despite the use of high-throughput screening methods. The challenge of rational excipient selection within ASD development timelines is key to the limited number of solid dispersions that reach the market (Walden et al., 2021). In this space, computational tools are gaining increasing attention as a complement to in vitro work and bridging knowledge gaps to support drug development. In the present work, the ranking obtained from the COSMO-RS calculations was compared to the experimentally observed precipitation inhibitory efficiency of the polymers. Assuming good alignment between computational and experimental data, future work could be limited to computational work to obtain an initial preselection of polymers. Therefore, the ranking obtained by COSMO-RS may be used as groundwork to narrow the list of polymers to be experimentally evaluated in the following steps. For this purpose, first the ASD release profiles, and PI-functionality of the polymers were assessed. As previously explained, only polymers that resulted in at least 80 % API release from the ASD were selected, in order to have comparable levels of supersaturation within ASDs with the same API. The polymers that showed no precipitation throughout the experiment were classified as precipitation inhibition-functional (PI-functional), indicating that these polymers effectively sustained supersaturation during the entire experiment. Secondly, the ASDs were ranked in order of increasing drug activity

Table 1
ASD, API, polymer and water content used for modeling purposes. API and polymer content together constitute the ASD amount finally present in water. The weight fraction (*w*) of the ternary sytem (API, polymer and water) add up to 1 (or 100%).

(1:2 w/w) API:Polymer				(1:3 w/w) API:Polymer			
ASD (*w*) in water	API (*w*)	Polymer (*w*)	Water (*w*)	ASD *w* in water	API (*w*)	Polymer (*w*)	Water (*w*)
0.01	0.0033	0.0066	0.99	0.01	0.0025	0.0075	0.99
0.05	0.0166	0.0333	0.95	0.05	0.0125	0.0375	0.95
0.10	0.0333	0.0666	0.90	0.10	0.0250	0.0750	0.90
0.15	0.0500	0.1000	0.85	0.15	0.0375	0.1125	0.85
0.20	0.0666	0.1333	0.80	0.20	0.0500	0.1500	0.80
0.25	0.0833	0.1666	0.75	0.25	0.0625	0.1875	0.75
0.30	0.1000	0.2000	0.70	0.30	0.0750	0.2250	0.70
0.35	0.1166	0.2333	0.65	0.35	0.0875	0.2625	0.65
0.40	0.1333	0.2666	0.60	0.40	0.1000	0.3000	0.60
0.45	0.1500	0.3000	0.55	0.45	0.1125	0.3375	0.55
0.50	0.1666	0.3333	0.50	0.50	0.1250	0.3750	0.50

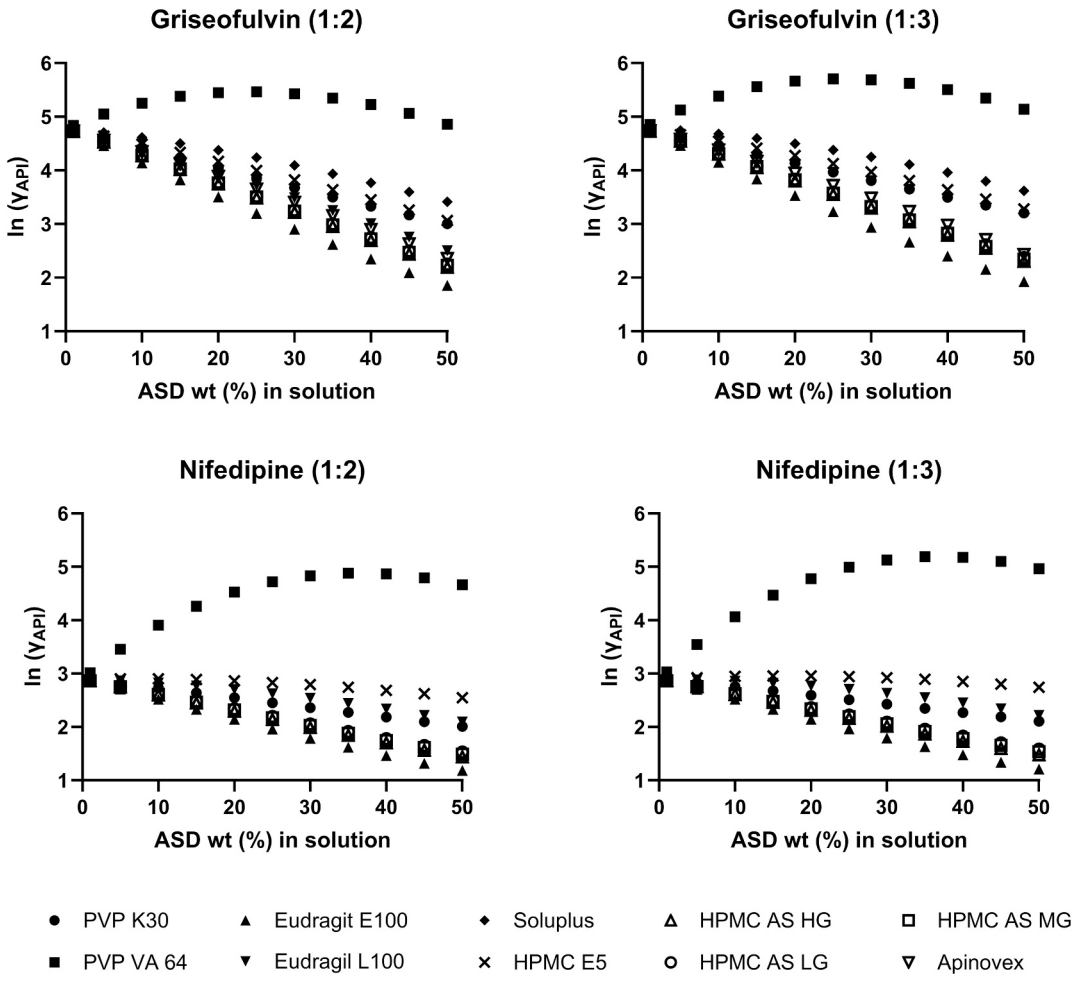

Fig. 4. Changes in activity coefficient/interaction strength as a consequence of increasing ASD present in solution.

coefficient, calculated by COSMO-RS. The results are presented in Tables 3a and 3b.

Assuming that a stronger drug-polymer interaction would align with efficient precipitation inhibition, one would expect all ASDs presenting a low activity coefficient also to show sustained supersaturation profiles. In contrast, ASDs with high activity coefficients, in the bottom part of the table, are likely to exhibit precipitation. This alignment expectation is shown in the last column of Tables 3a and 3b. If the polymer was found to be a good PI experimentally, and this was supported by the COSMO-RS calculations (i.e. it had a low activity coefficient), good alignment between experiments and calculations was assumed.

Despite none of the system shows negative ln (γ_{API}), it is possible to provide a qualitative ranking. A natural separation is evident between the polymers in the upper and lower parts of the table, where the first polymer to exhibit precipitation acts as a dividing line between the two groups. Accordingly, ln (γ_{API}) for the systems above Apinovex should be lower, than for the ones below it. For example, for Griseofulvin ASDs the first polymer to exhibit precipitation is Apinovex at both the 1:2 w/w and 1:3 w/w API:polymer ratios. It can be seen that the COSMO-RS rankings largely aligned with the polymer PI-functionality observed during the release experiments, in that ln (γ_{API}) of the API for the ASD systems above Apinovex was lower, and therefore sustained precipitation efficiently, while the ones with a higher ln (γ_{API}), below Apinovex in the Table 3a, exhibited precipitation. Alignment between experimental and computational data was observed in 84 % of the cases for griseofulvin and 87 % of the cases for nifedipine; only a small number of polymers deviated from the COSMO-RS ranking. This strong alignment supported the approach to compare in silico and experimental results in a drug-specific way, separated for given drug to polymer ratios. Cases where the COSMO-RS calculations did not align with observed PI-functionality in the release experiments can be accounted for by different mechanisms. Firstly, it should be considered that COSMO-RS is a thermodynamic model, which does not directly account for kinetic effects exerted by the polymer. Nevertheless, calculated activity coefficients are likely related to those kinetic effects that are affected by molecular drug-polymer interactions. However, ASD dissolution is a very complex process. A simple evaluation of drug-polymer interaction strength may sometimes be insufficient—even in a solvent-shift PI experiment with predissolved drug and polymer—to fully explain the data. Despite of such simplification, a previous study found at least a ranking correlation between binary drug-excipient excess enthalpy calculations and PI performance (Price et al., 2019). Release kinetics of solvent-cased ASDs is considerably more complex, owing to the formation of a hydration layer where drug-rich phases may occur with non-crystalline and/or crystalline drug separation (Ricarte et al., 2019). Moreover, the crystallization tendency of the API itself (i.e., its glass forming ability) has been shown to affect ASD release profiles greatly (Blaabjerg et al., 2018). These drug-specific effects in the hydration layer were shown to influence both release kinetics and supersaturation behavior (Li and Taylor, 2019; Ricarte et al., 2019). Another mechanism is that nanoaggregates may form due to interactions between dissolution medium components or from the aggregation of polymeric chains. These aggregated polymer chains can create a micellar corona that interacts non-covalently with the drug, preventing precipitation and acting as a reservoir to help sustain supersaturation levels (Li et al., 2018; Ricarte et al., 2019). High drug concentrations in the hydration layer or bulk can

Table 2
Ranking of ASDs based on the calculated (COSMO-RS) drug activity coefficient (ln γ_{API}) for 1% (w/w) and 50% (w/w) ASD content in solution to reflect different stages of formulation dilution/dispersion. ASDs are ranked in order of decreasing interaction strength.

Griseofulvin

1/2 ASD				1/3 ASD			
1 % ASD in solution	ln (γAPI)	50 % ASD in solution	ln (γAPI)	1 % ASD in solution	ln (γAPI)	50 % ASD in solution	ln (γAPI)
Eudragit E100	4.714	Eudragit E100	1.857	Eudragit E100	4.715	Eudragit E100	1.926
HPMC AS HG	4.727	HPMC AS HG	2.195	HPMC AS HG	4.73	HPMC AS HG	2.307
HPMC AS MG	4.728	HPMC AS MG	2.228	HPMC AS MG	4.731	HPMC AS MG	2.344
HPMC AS LG	4.729	HPMC AS LG	2.254	HPMC AS LG	4.732	HPMC AS LG	2.374
Apinovex	4.735	Apinovex	2.358	Apinovex	4.738	Apinovex	2.433
Eudragit L100	4.738	Eudragit L100	2.504	PVP K30	4.748	PVP K30	3.206
PVP K30	4.744	PVP K30	3.008	HPMC E5	4.755	HPMC E5	3.28
HPMC E5	4.75	HPMC E5	3.067	Soluplus	4.772	Soluplus	3.621
Soluplus	4.765	Soluplus	3.417	PVP VA 64	4.855	PVP VA 64	5.142
PVP VA 64	4.838	PVP VA 64	4.862	Eudragit L100	4.855	Eudragit L100	5.142

Nifedipine

1/2 ASD				1/3 ASD			
1 % ASD in solution	**ln (γAPI)**	**50 % ASD in solution**	**ln (γAPI)**	**1 % ASD in solution**	**ln (γAPI)**	**50 % ASD in solution**	**ln (γAPI)**
Eudragit E100	2.855	Eudragit E100	1.185	Eudragit E100	2.855	Eudragit E100	1.21
HPMC AS HG	2.863	HPMC AS HG	1.439	HPMC AS HG	2.864	HPMC AS HG	1.477
HPMC AS MG	2.864	HPMC AS MG	1.491	HPMC AS MG	2.865	HPMC AS MG	1.537
HPMC AS LG	2.865	HPMC AS LG	1.533	HPMC AS LG	2.866	HPMC AS LG	1.586
PVP K30	2.878	PVP K30	2.011	PVP K30	2.88	PVP K30	2.107
Apinovex	2.884	Eudragit L100	2.093	Apinovex	2.888	Eudragit L100	2.22
Eudragit L100	2.887	Apinovex	2.142	Eudragit L100	2.89	Apinovex	2.245
HPMC E5	2.894	HPMC E5	2.549	HPMC E5	2.899	HPMC E5	2.746
Soluplus	2.917	Soluplus	2.884	Soluplus	2.924	Soluplus	3.073
PVP VA 64	3.013	PVP VA 64	4.664	PVP VA 64	3.033	PVP VA 64	4.965

Table 3a
Calculated drug activity coefficient (ln (γ_{API})) in the studied ASDs containing griseofulvin and alignment to polymer precipitation inhibition (PI-functionality observed during dissolution experiments.

Griseofulvin:polymer (1:2 w/w)				
Ranking	Polymer	ln (γ_{API})	PI-FunctionalY/N	Experiment/COSMO-RS alignment?Y/N
1	Eudragit E100	4.713	Y	Y
2	HPMC AS HG	4.727	Y	Y
3	HPMC AS MG	4.728	Y	Y
4	HPMC AS LG	4.728	Y	Y
5	Apinovex	4.734	N	Y
6	Eudragit L100	4.738	N	Y
7	PVP K30	4.743	N	Y
8	HPMC E5	4.749	Y	N
9	Soluplus	4.764	Y	N
10	PVP VA 64	4.838	N	Y

Griseofulvin:polymer (1:3 w/w)				
1	Eudragit E100	4.715	Y	Y
2	HPMC AS HG	4.73	Y	Y
3	HPMC AS MG	4.731	Y	Y
4	HPMC AS LG	4.732	Y	Y
5	Apinovex	4.738	N	Y
6	PVP K30	4.748	N	Y
7	HPMC E5	4.755	Y	N
8	Soluplus	4.772	Y	N
9	PVP VA 64	4.855	N	Y

Table 3b
Calculated drug activity coefficient (ln (γ_{API})) in the studied ASDs containing nifedipine and alignment to polymer precipitation inhibition (PI-functionality observed during dissolution experiments.

Nifedipine:polymer (1:2 w/w)				
Ranking	Polymer	ln (γ_{API})	PI-Functional Y/N	Experiment/COSMO-RS alignment? Y/N
1	Eudragit E100	2.855	Y	Y
2	HPMC AS HG	2.863	Y	Y
3	HPMC AS MG	2.864	Y	Y
4	HPMC AS LG	2.865	Y	Y
5	PVP K30	2.878	N	Y
6	Eudragit L100	2.887	N	Y
7	HPMC E5	2.894	Y	N
8	PVP VA 64	3.013	N	Y

Nifedipine:polymer (1:3 w/w)				
1	Eudragit E100	2.855	Y	N
2	HPMC AS HG	2.864	Y	Y
3	HPMC AS MG	2.865	Y	Y
4	HPMC AS LG	2.866	Y	Y
5	PVP K30	2.88	N	Y
6	Eudragit L100	2.89	N	N
7	HPMC E5	2.899	Y	N
8	PVP VA 64	3.033	N	Y

exceed that of the amorphous solubility leading to a liquid–liquid phase separation (LLPS) (Indulkar et al., 2015). This process can cause the drug-rich phase that is particularly observed in the hydration layer. This drug rich phase can also act as a reservoir to maintain supersaturation (Indulkar et al., 2016). Any supramolecular effects between drug and polymer in the bulk phase pose a challenge for thermodynamic modeling. Thus, effects such as nesting of the drug within coiled polymer chains cannot be captured at present by the COSMO-RS model, but would influence the experimentally observed supersaturation maintenance. Such supramolecular and other colloidal effects can be observed with molecular simulations (Zeneli et al., 2024). However, these full-atomistic simulations are very time-consuming at larger scales, making coarse-grained (CG) modeling a necessity. Such a CG simulation approach has recently been combined with thermodynamic modeling to describe the hydration layer of ASDs (Walter et al., 2024), although this modeling research is still at an early stage and therefore, at least for now, less useful for early screening purposes. Given the complexity of the ASD release mechanisms, the calculated drug activity coefficients by means of COSMO-RS theory and the ranking of the experimentally observed release curves, were deemed to be in fairly good agreement. This makes the proposed combined in vitro-in silico approach a viable option for early ASD screening.

4. Conclusions

ASDs of two different APIs in the presence of ten pharmaceutically relevant polymers, at different ratios, were investigated for their release and supersaturation maintenance performance. The experimental results were compared to drug activity coefficient calculations obtained by COSMO-RS theory. The calculations were in very good alignment with the PI-functionality of the polymers. Alignment between experimental and computational data was observed in 84 % of the cases for griseofulvin and 87 % of the cases for nifedipine. For the ASDs that deviated from the alignment with the computed drug activity coefficients, complex ASD dissolution behavior and the hydration dynamics of the gel layer may be the leading cause. Important to note is therefore that the simplifying view on computed activity coefficients based on COSMO-RS theory has at least for now limitations when more complex kinetic effects of mesoscopic structuring occur in the process of drug release from ASDs. Additionally, the crystallization tendency of the API itself can greatly affect release ASD profiles and consequently the potential for PI-performance is drug-specific. While more experiments would corroborate with the proposed screening strategy, the present study, together with previous work on the physical instability performance of ASDs, provides insights and proposes an initial computational approach to aid excipient selection based on the drug activity coefficient obtained from COSMO-RS. This strategy accelerates the pre-formulation screening processes targeted at excipient selection by relying on computational and automated miniaturized experiments.

CRediT authorship contribution statement

Egis Zeneli: Writing – review & editing, Writing – original draft, Investigation, Formal analysis, Data curation, Conceptualization. **Hugo Bohets:** Supervision, Methodology, Conceptualization. **Frédéric Ngono Mebenga:** Supervision, Methodology, Conceptualization. **Christophe Tistaert:** Supervision, Conceptualization. **René Holm:** Writing – review & editing, Supervision. **Martin Kuentz:** Writing – review & editing, Supervision, Funding acquisition.

Declaration of competing interest

The authors declare that they have no known competing financial interests or personal relationships that could have appeared to influence the work reported in this paper.

Acknowledgement

This project has received funding from the European Union's Horizon 2020 research and innovation program under the Marie Skłodowska-Curie grant agreement No. 955756.

Andrew Brown is gratefully acknowledged for his valuable proofreading of the final manuscript.

Data availability

Data will be made available on request.

References

Adhiyaman, R., Basu, S.K., 2006. Crystal modification of dipyridamole using different solvents and crystallization conditions. Int. J. Pharm. 321, 27–34.
Alopaeus, J. F. H., E.Tho, I. 2019. Micellisation mechanism and behaviour of soluplus®–furosemide micelles: Preformulation studies of an oral nanocarrier-based system. MDPI AG.
Alhalaweh, A., Alzghoul, A., Mahlin, D., Bergstrom, C.A.S., 2015. Physical stability of drugs after storage above and below the glass transition temperature: relationship to glass-forming ability. Int. J. Pharm. 495, 312–317.
Antolovic, I., Vrabec, J., Klajmon, M., 2024. COSMOPharm: drug-polymer compatibility of pharmaceutical amorphous solid dispersions from COSMO-SAC. Mol. Pharm. 21, 4395–4415.
Aulifa, D.L., Al shofwan, A.A., Megantara, S., Fakih, T.M., Budiman, A., 2024. Elucidation of molecular interactions between drug-polymer in amorphous solid dispersion by a computational approach using molecular dynamics simulations. Adv. Appl. Bioinform. Chem. 17, 1–19.
Baird, J.A., Taylor, L.S., 2012. Evaluation of amorphous solid dispersion properties using thermal analysis techniques. Adv. Drug Deliv. Rev. 64, 396–421.
Baird, J.A., van Eerdenbrugh, B., Taylor, L.S., 2010. A classification system to assess the crystallization tendency of organic molecules from undercooled melts. J. Pharm. Sci. 99, 3787–3806.
Becke, A.D., 1988. Density-functional exchange-energy approximation with correct asymptotic behavior. Phys. Rev. A Gen. Phys. 38, 3098–3100.
Bhujbal, S.V., Mitra, B., Jain, U., Gong, Y., Agrawal, A., Karki, S., Taylor, L.S., Kumar, S., Tony Zhou, Q., 2021. Pharmaceutical amorphous solid dispersion: a review of manufacturing strategies. Acta Pharm. Sin. B 11, 2505–2536.
Blaabjerg, L.I., Lindenberg, E., Lobmann, K., Grohganz, H., Rades, T., 2018. Is there a correlation between the glass forming ability of a drug and its supersaturation propensity? Int. J. Pharm. 538, 243–249.
Butreddy, A., 2022. Hydroxypropyl methylcellulose acetate succinate as an exceptional polymer for amorphous solid dispersion formulations: a review from bench to clinic. Eur. J. Pharm. Biopharm. 177, 289–307.
Chauhan, H., Hui-Gu, C., Atef, E., 2013. Correlating the behavior of polymers in solution as precipitation inhibitor to its amorphous stabilization ability in solid dispersions. John Wiley and Sons Inc.
Chavan, R.B., Thipparaboina, R.K., Dinesh, Shastri, N.R., 2016. Evaluation of the inhibitory potential of HPMC, PVP and HPC polymers on nucleation and crystal growth. Royal Society of Chemistry.
Chen, Y., Wang, S., Wang, S., Liu, C., Su, C., Hageman, M., Hussain, M., Haskell, R., Stefanski, K., Qian, F., 2016. Initial drug dissolution from amorphous solid dispersions controlled by polymer dissolution and drug-polymer interaction. Pharm. Res. 33, 2445–2458.
Chiang, P.C., Ran, Y., Chou, K.J., Cui, Y., Sambrone, A., Chan, C., Hart, R., 2012. Evaluation of drug load and polymer by using a 96-well plate vacuum dry system for amorphous solid dispersion drug delivery. AAPS PharmSciTech 13, 713–722.
Dai, W.G., Dong, L.C., Li, S., Pollock-Dove, C., Chen, J., Mansky, P., Eichenbaum, G., 2007. Parallel screening approach to identify solubility-enhancing formulations for improved bioavailability of a poorly water-soluble compound using milligram quantities of material. Int. J. Pharm. 336, 1–11.
Diedenhofen, M., Klamt, A., 2010. COSMO-RS as a tool for property prediction of IL mixtures—a review. Fluid Phase Equilib. 294, 31–38.
Ding, Y., Cui, W., Zhang, Z., Ma, Y., Ding, C., Lin, Y., Xu, Z., 2023. Solubility and pharmacokinetic profile improvement of griseofulvin through supercritical carbon dioxide-assisted complexation with hp-gamma-cyclodextrin. Molecules 28.
Ditzinger, F., Wieland, R., Statelova, M., Vertzoni, M., Holm, R., Kuentz, M., 2020. In vivo performance of innovative polyelectrolyte matrices for hot melt extrusion of amorphous drug systems. Mol. Pharm. 17, 3053–3061.
Fdukeck, R., Sieger, P., Karmwar, P., 2013. Investigation and correlation of physical stability, dissolution behaviour and interaction parameter of amorphous solid dispersions of telmisartan: a drug development perspective. Eur. J. Pharm. Sci. 49, 723–731.
Frank, D.S., Prasad, P., Iuzzolino, L., Schenck, L., 2022. Dissolution behavior of weakly basic pharmaceuticals from amorphous dispersions stabilized by a poly (dimethylaminoethyl methacrylate) copolymer. Mol. Pharm. 19, 3304–3313.
Gao, P., Akrami, A., Alvarez, F., Hu, J., Li, L., Ma, C., Surapaneni, S., 2009. Characterization and optimization of AMG 517 supersaturatable self-emulsifying drug delivery system (S-SEDDS) for improved oral absorption. J. Pharm. Sci. 98, 516–528.

Guzman, H.R., Tawa, M., Zhang, Z., Ratanabanangkoon, P., Shaw, P., Gardner, C.R., Chen, H., Moreau, J.P., Almarsson, O., Remenar, J.F., 2007. Combined use of crystalline salt forms and precipitation inhibitors to improve oral absorption of celecoxib from solid oral formulations. J. Pharm. Sci. 96, 2686–2702.

Han, J., Tang, M., Yang, Y., Sun, W., Yue, Z., Zhang, Y., Zhu, Y., Liu, X., Wang, J., 2023. Amorphous solid dispersions: Stability mechanism, design strategy and key production technique of hot melt extrusion. Int. J. Pharm. 646, 123490.

Indulkar, A.S., Box, K.J., Taylor, R., Ruiz, R., Taylor, L.S., 2015. pH-dependent liquid-liquid phase separation of highly supersaturated solutions of weakly basic drugs. Mol. Pharm. 12, 2365–2377.

Indulkar, A.S., Gao, Y., Raina, S.A., Zhang, G.G., Taylor, L.S., 2016. Exploiting the phenomenon of liquid-liquid phase separation for enhanced and sustained membrane transport of a poorly water-soluble drug. Mol. Pharm. 13, 2059–2069.

Kawakami, K., 2012. Modification of physicochemical characteristics of active pharmaceutical ingredients and application of supersaturatable dosage forms for improving bioavailability of poorly absorbed drugs. Adv. Drug Deliv. Rev. 64, 480–495.

Klamt, A., 2011. The COSMO and COSMO-RS solvation models. WIREs Comput. Mol. Sci. 1, 699–709.

Klamt, A., Eckert, F., 1999. COSMORS : a novel and efficient method for the a priori prediction. Fluid Phase Equilib. 172, 43–72.

Knopp, M.M., Nguyen, J.H., Mu, H., Langguth, P., Rades, T., Holm, R., 2016. Influence of copolymer composition on in vitro and in vivo performance of celecoxib-PVP/VA amorphous solid dispersions. AAPS J. 18, 416–423.

Leopold, C.S., Eikeler, D., 1997. Eudragit@ E as coating material for the pH-controlled drug release in the topical treatment of inflammatory bowel disease (IBD). J. Drug Target. 6, 85–94.

Li, N., Taylor, L.S., 2019. Microstructure formation for improved dissolution performance of lopinavir amorphous solid dispersions. Mol. Pharm. 16, 1751–1765.

Li, Z., Lenk, T.I., Yao, L.J., Bates, F.S., Lodge, T.P., 2018. Maintaining hydrophobic drug supersaturation in a micelle corona reservoir. Macromolecules 51, 540–551.

Linares, V., Yarce, C.J., Echeverri, J.D., Galeano, E., Salamanca, C.H., 2019. Relationship between degree of polymeric ionisation and hydrolytic degradation of Eudragit((R)) E polymers under extreme acid conditions. Polym. (basel) 11.

Niederquell, A., Herzig, S., Schonenberger, M., Stoyanov, E., Kuentz, M., 2024. Computational support to explore ternary solid dispersions of challenging drugs using coformer and hydroxypropyl cellulose. Mol. Pharm. 21, 5619–5631.

Perdew, J.P., 1986. Density-functional approximation for the correlation energy of the inhomogeneous electron gas. Phys. Rev. B Condens. Matter 33, 8822–8824.

Plumley, C., Gorman, E.M., El-Gendy, N., Bybee, C.R., Munson, E.J., Berkland, C., 2009. Nifedipine nanoparticle agglomeration as a dry powder aerosol formulation strategy. Int. J. Pharm. 369, 136–143.

Price, D.J., Nair, A., Kuentz, M., Dressman, J., Saal, C., 2019. Calculation of drug-polymer mixing enthalpy as a new screening method of precipitation inhibitors for supersaturating pharmaceutical formulations. Eur. J. Pharm. Sci. 132, 142–156.

Que, C., Deac, A., Zemlyanov, D.Y., Qi, Q., Indulkar, A.S., Gao, Y., Zhang, G.G.Z., Taylor, L.S., 2021. Impact of drug-polymer intermolecular interactions on dissolution performance of copovidone-based amorphous solid dispersions. Mol. Pharm. 18, 3496–3508.

Ricarte, R.G., van Zee, N.J., Li, Z., Johnson, L.M., Lodge, T.P., Hillmyer, M.A., 2019. Recent advances in understanding the micro- and nanoscale phenomena of amorphous solid dispersions. Mol. Pharm. 16, 4089–4103.

Rumondor, A.C., Stanford, L.A., Taylor, L.S., 2009. Effects of polymer type and storage relative humidity on the kinetics of felodipine crystallization from amorphous solid dispersions. Pharm. Res. 26, 2599–2606.

Schram, C.J., Beaudoin, S.P., Taylor, L.S., 2015. Impact of polymer conformation on the crystal growth inhibition of a poorly water-soluble drug in aqueous solution. Langmuir 31, 171–179.

Shanbhag, A., Rabel, S., Nauka, E., Casadevall, G., Shivanand, P., Eichenbaum, G., Mansky, P., 2008. Method for screening of solid dispersion formulations of low-solubility compounds–miniaturization and automation of solvent casting and dissolution testing. Int. J. Pharm. 351, 209–218.

Taylor, L.S.Z., Geoff, G.Z., 2016. Physical chemistry of supersaturated solutions and implications for oral absorption. Elsevier B.V.

Walden, D.M., Bundey, Y., Jagarapu, A., Antontsev, V., Chakravarty, K., Varshney, J., 2021. Molecular simulation and statistical learning methods toward predicting drug-polymer amorphous solid dispersion miscibility, stability, and formulation design. Molecules 26.

Walter, S., Mileo, P.G.M., Afzal, M.A.F., Kyerematen, S.O., Degenhardt, M., Browning, A.R., Shelley, J.C., 2024. Predicting the release mechanism of amorphous solid dispersions: a combination of thermodynamic modeling and in silico molecular simulation. Pharmaceutics 16.

Warren, D.B., Benameur, H., Porter, C.J., Pouton, C.W., 2010. Using polymeric precipitation inhibitors to improve the absorption of poorly water-soluble drugs: a mechanistic basis for utility. J. Drug Target. 18, 704–731.

Wolbert, F., Fahrig, I.K., Gottschalk, T., Luebbert, C., Thommes, M., Sadowski, G., 2022. Factors influencing the crystallization-onset time of metastable ASDs. Pharmaceutics 14.

Wyttenbach, N., Janas, C., Siam, M., Lauer, M.E., Jacob, L., Scheubel, E., Page, S., 2013. Miniaturized screening of polymers for amorphous drug stabilization (SPADS): rapid assessment of solid dispersion systems. Eur. J. Pharm. Biopharm. 84, 583–598.

Xiang, T.X., Anderson, B.D., 2014. Molecular dynamics simulation of amorphous hydroxypropyl-methylcellulose acetate succinate (HPMCAS): polymer model development, water distribution, and plasticization. Mol. Pharm. 11, 2400–2411.

Zeneli, E., Bohets, H., Mebenga, F.N., Holm, R., Tistaert, C., Kuentz, M., 2025. Guiding excipient selection for physically stable amorphous solid dispersions: a combined in-vitro in-silico approach. Eur. J. Pharm. Sci., 107152

Zeneli, E., Lange, J.J., Holm, R., Kuentz, M., 2024. A study of hydrophobic domain formation of polymeric drug precipitation inhibitors in aqueous solution. Eur. J. Pharm. Sci. 198, 106791.

Zhang, S., Lee, T.W.Y., Chow, A.H.L., 2019. Thermodynamic and kinetic evaluation of the impact of polymer excipients on storage stability of amorphous itraconazole. Int. J. Pharm. 555, 394–403.